Electron-Beam-Induced Color Imaging of Acid-Chromic Polymer Films

Yasunari Maekawa,*,† Kanako Yuasa,†,‡ Kazuyuki Enomoto,† Harumi Matsushita,‡ Jun Kato,‡ Takashi Yamashita,‡ Kazuo Itoh,§ and Masaru Yoshida†

Conducting Polymer Materials Group, Environment and Industrial Materials Research Division, Quantum Beam Science Directorate, Japan Atomic Energy Agency (JAEA), 1233 Watanuki, Takasaki, Gunma 370-1292, Japan, Department of Pure and Applied Chemistry, Tokyo University of Science, 2641 Yamazaki, Noda, Chiba 278-8510 Japan, and Department of Electronic Engineering, Faculty of Engineering, Gunma University, 1-5-1 Tenjin, Kiryu, Gunma 376-8515, Japan

Received March 6, 2008. Revised Manuscript Received May 20, 2008

Polymer films with acid-responsive chromic dyes and acid generators have been designed for an electron-beam (EB)-induced color imaging system. Arylsulfonic acid esters and triphenylsulfonium salts were used as an EB-sensitive acid generator; the acid (H^+) allows a chromic reaction with rhodamine B base (**RB**) and 4,4′-bis(dimethylamino)benzhydrol (**BH**) to be triggered. Upon EB irradiation, poly(methyl methacrylate) (PMMA) films consisting of **RB** or **BH** and acid generators exhibited a characteristic absorption band with λ_{max} at 560 and at 612 nm, respectively, and an isosbestic point. These spectral changes clearly indicate that colorless chromic dyes in PMMA are transformed selectively to the colored form. The color imaging of these films was performed by electron-beam direct writing (EBDW) with a 50 nm diameter beam to form 100−1000 nm line and space patterns and evaluated by optical and confocal laser microscopy. EBDW on the acid-chromic polymer films, especially for **BH**, yielded clear color imaging of 100−200 nm line and space patterns with a dose of only 10 μC cm^{-2}. Confocal laser microscopy gave thinner lines than the laser wavelength (632.8 nm), probably because of the large change in refractive index of the patterned film induced by EB irradiation even with a low-energy dose.

Introduction

Ionizing radiation such as X-rays (EUV), electron beams (EB), and ion beams has attracted great attention as a future lithographic tool and also as a promising technique for fabricating nanoscale electronic devices by virtue of its extremely short wavelength.[1–3] This is a way to overcome optical resolution limitations of UV and visible light due to their wavelength. The electron-beam direct writing (EBDW) technique is now quite advanced with resolution down to sub-10 nm, which would be impossible to achieve with light, and thus should be applicable to high-density recording devices.[4–12] The major requirement of EB for recording devices is the EB-induced chemical changes providing optical or reflective-index differentiation between the exposed and unexposed regions. Although design and search for highly EB-sensitive materials are required for realizing such devices, little is known of the EB radiolysis of potential materials.[13–15]

We previously reported on the EB-induced reactions of cinnamic acid derivatives,[16] sulfonium salts,[17–19] and sulfonic acid derivatives,[20–22] which are well known to be photosensitive materials. The product studies show that both arylsulfonic acid esters and sulfonium salts are highly EB-sensitive compounds producing an acid (H^+) efficiently; such acid

* To whom correspondence should be addressed. E-mail: maekawa.yasunari@jaea.go.jp.
† Japan Atomic Energy Agency.
‡ Tokyo University of Science.
§ Gunma University.

(1) Sheats, J. R.; Smith, B. W. *Microlithography, Science and Technology*; Marcel Dekker Inc.: New York, 1998.
(2) Wallraff, G. M.; Hinsberg, W. D. *Chem. Rev.* **1999**, *99*, 1801–1821.
(3) Brainard, R. L.; Barclay, G. G.; Anderson, E. H.; Ocola, L. E. *Microelectron. Eng.* **2002**, *61−62*, 707–715.
(4) Brack, H.-P.; Padeste, C.; Slaski, M.; Alkan, S.; Solak, H. H. *J. Am. Chem. Soc.* **2004**, *126*, 1004–1005.
(5) Mendes, P. M.; Jacke, S.; Critchley, K.; Plaza, J.; Chen, Y.; Nikitin, K.; Palmer, R. E.; Preece, J. A.; Evans, S. D.; Fitzmaurice, D. *Langmuir* **2004**, *20*, 3766–3768.
(6) Russell, M. T.; Pingree, L. S. C.; Hersam, M. C.; Marks, T. J. *Langmuir* **2006**, *22*, 6712–6718.
(7) Wada, Y.; Katsumura, M.; Kojima, Y.; Kitahara, H.; Iida, T. *Jpn. J. Appl. Phys.* **2001**, *40*, 1653–1660.
(8) Hosaka, S.; Sano, H.; Itoh, K.; Sone, H. *Microelectron. Eng.* **2006**, *83*, 792–795.
(9) Irie, M. *Chem. Rev.* **2000**, *100*, 1685–1716.
(10) Berkovic, G.; Krongauz, V.; Weiss, V. *Chem. Rev.* **2000**, *100*, 1741–1753.
(11) Kaburagi, Y.; Tokita, S.; Kaneko, M. *Chem. Lett.* **2003**, *32*, 888–889.
(12) Scaiano, J. C.; Laferriere, M.; Ivan, M. G.; Taylor, G. N. *Macromolecules* **2003**, *36*, 6692–6694.
(13) Farhataziz, M.; Rodgers, A. J. *Radiation Chemistry, Principles and Applications*; VCH Publishers: New York, 1987.
(14) Tabata, Y.; Ito, Y.; Tagawa, S. *Handbook of Radiation Chemistry*; Tabata, Y., Ed.; CRC Press: Boca Raton, 1991.
(15) Hummel, A. In *Advances in Radiation Chemistry*; Burton, M., Magee, J. L., Eds.; John Wiley & Sons: New York, 1974; Vol. 4, pp 1−102.
(16) Maekawa, Y.; Inaba, T.; Hobo, H.; Narita, T.; Koshikawa, H.; Moon, S.; Kato, J.; Yoshida, M. *Chem. Commun.* **2002**, 2088–2089.
(17) Enomoto, K.; Moon, S.; Maekawa, Y.; Shimoyama, J.; Goto, K.; Narita, T.; Yoshida, M. *J. Vac. Sci. Technol. B* **2006**, *24*, 2337–2349.
(18) Enomoto, K.; Moon, S.; Maekawa, Y.; Shimoyama, J.; Goto, K.; Narita, T.; Yoshida, M. *J. Photopolym. Sci. Technol.* **2004**, *17*, 41–44.
(19) Moon, S.; Maekawa, Y.; Yoshida, M. *Chem. Lett.* **2001**, 408–409.
(20) Yuasa, K.; Enomoto, K.; Maekawa, Y.; Kato, J.; Yamashita, T.; Yoshida, M. *J. Photopolym. Sci. Technol.* **2004**, *17*, 21–28.
(21) Kato, J.; Maekawa, Y.; Yoshida, M. *Chem. Lett.* **2005**, *34*, 266–267.
(22) Kato, J.; Kakehata, H.; Maekawa, Y.; Yamashita, T. *Chem. Commun.* **2006**, 4498–4500.

10.1021/cm800650q CCC: $40.75
Published on Web 08/06/2008

generators could be applied to producing a nanoscale device.[23–25] The EB radiolysis of sulfonamide derivatives in the crystalline state causes the Fries rearrangement and scission which creates aniline derivatives. This rearrangement is accompanied by transformation from acidic sulfonamides to basic anilines.[20,21] Recently, the above reactions have been induced by EB in polymeric systems, designing polysulfonamide films in which the sulfonamide groups are converted to aniline groups in the main chain and at the polymer terminal. Since the generated aniline groups can be transformed with Ehrlich's reagent into colored aromatic imines, this EB-sensitive polysulfonamide film can be patterned with nanoscale resolution by EBDW and successive color-forming reactions.[26]

Herein we report on novel color-forming polymer films for nanoscale imaging by EBDW. The thin poly(methyl methacrylate) (PMMA) films, consisting of acid-chromic dyes and acid generators, were employed for EB-induced color formation as depicted in Scheme 1. Arylsulfonic acid esters and triphenylsulfonium salts were used as the acid generator; the acid (H^+) allows the reaction to be triggered. The acid-chromic dyes employed here, rhodamine B base (**RB**) and 4,4′-bis(dimethylamino)benzhydrol (**BH**), react with the acid and thus are colored without post-treatment such as additional color-forming chemical reactions and thermal transformations.[27–31] The color imaging of these films was performed by EBDW to form 100−1000 nm line and space patterns and evaluated by optical and confocal laser microscopy.

Scheme 1. (Top) EB-Induced Color-Imaging Process for Acid-Induced Color Change Polymer Films (for details, see text). (Middle) Chemical Structures of Acid Generators Used. (Bottom) Acid-Induced Color Change Reactions for Rhodamine B Base (RB) and 4,4′-Bis(dimethylamino)benzhydrol (BH)

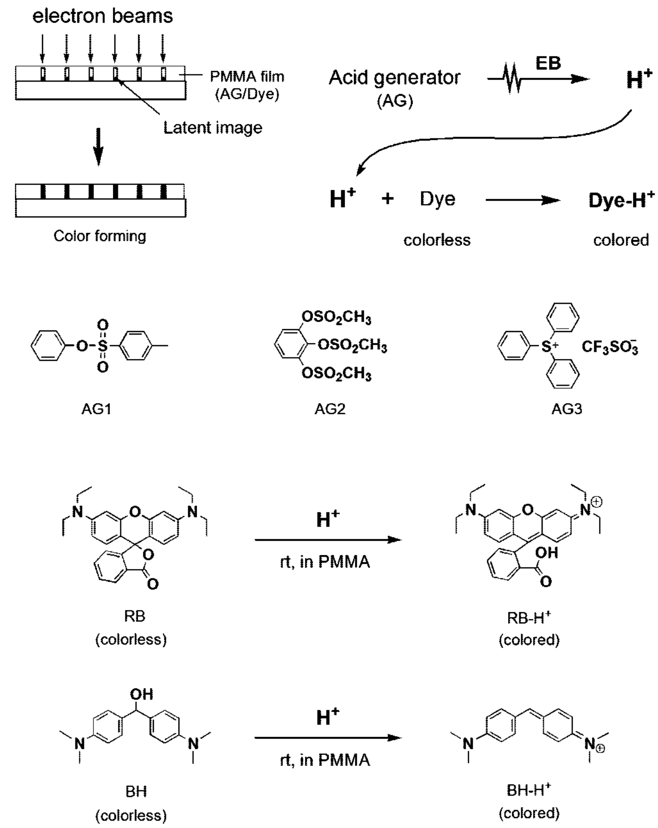

Experimental Section

Materials. RB, **BH**, **AG3**, and PMMA, 15 K, were purchased from Aldrich and purified by standard procedures. **AG1** was obtained from Tokyo Chemical Industry and purified by recrystallization from methanol. **AG2** was obtained from Midori Kagaku and used as received. Other organic solvents used were of commercial quality unless otherwise stated.

EB-Induced Acid Chromism. A solution containing 15 wt % PMMA in 85 wt % cyclohexanone and 2-ethoxyethanol (2:1 vol./vol.) as a solvent and 1 − 3 wt % acid-chromic dyes (relative to PMMA) with an equimolar or 3-fold molar amount (relative to a chromic dye) of EB-acid generator were filtered through a 0.22 μm Millipore Millex filter. The filtrate was spin coated onto previously cleaned quartz at 800 rpm for 10 s and 1800 rpm for 20 s and baked at 90 °C on a hot plate for 3 min to form a 0.6−0.8 μm thick film. The thickness of those thin films was measured by scanning the film surface using a Mitutoyo Surftest SV-600 surface roughness tester. EB irradiation of the films was carried out using a cascade-type electron accelerator (Dynamitron) or a Cockcroft-Walton-type electron accelerator at JAEA Takasaki. The film thus cast on quartz was then covered with a Kapton film and irradiated with EB (accelerating voltage, 1 MeV; beam current, 0.5 mA) on a water-cooled plate in air at ambient temperature. Dose-dependent studies were performed with exposure doses up to 200 μC cm^{-2}. Colorations due to acid chromism triggered by EB were evaluated using a HITACHI U-3210 UV−visible spectrometer. Refractive index measurement was carried out by an m-line method. An incident light source of 632.8 nm (He−Ne laser) was used.[32,33]

EB-Induced Color Imaging. A solution containing 15 wt % PMMA in 85 wt % mixed solution of cyclohexanone and 2-ethoxyethanol (2:1 vol./vol.) as a solvent, 1−3 wt % chromic dyes (relative to PMMA), and equimolar or 3-fold molar EB-acid generator (relative to the chromic dye) were filtered through a 0.22 μm Millipore Millex filter. The filtrate was spin coated onto a previously cleaned Si wafer at 3000 rpm for 40 s, baked at 90 °C on a hot plate for 3 min, and then dried in vacuo. The thickness of the films obtained was 0.35 μm. The film was then exposed with a raster scanning EB using the JSM-5310W Tokyo Technology Beam Draw System. The accelerating voltage of the incident electron beam was

(23) Szmanda, C. R.; Brainard, R. L.; Mackevich, J. F.; Awaji, A.; Tanaka, T.; Yamada, Y.; Bohland, J.; Tedesco, S.; Dal'Zotto, B.; Bruenger, W.; Torkler, M.; Fallmann, W.; Loeschner, H.; Kaesmaier, R.; Nealey, P. M.; Pawloski, A. R. *J. Vac. Sci. Technol. B* **1999**, *172*, 3356–3361.
(24) Yamamoto, H.; Kozawa, T.; Nakano, A.; Okamoto, K.; Tagawa, S.; Ando, T.; Sato, M.; Komano, H. *J. Vac. Sci. Technol. B* **2004**, *22*, 3522–3524.
(25) Kozawa, T.; Shigaki, T.; Okamoto, K.; Saeki, A.; Tagawa, S.; Kai, T.; Shimokawa, T. *J. Vac. Sci. Technol. B* **2006**, *24*, 3055–3060.
(26) Maekawa, Y.; Kato, J.; Katakai, M.; Ishihara, M.; Enomoto, K.; Hagiwara, T.; Ishii, T.; Itoh, K.; Koshikawa, H.; Yoshida, M. *Macromol. Chem. Phys.* **2008**, *209*, 625–633.
(27) Pohlers, G.; Scaiano, J. C.; Sinta, R. *Chem. Mater.* **1997**, *9*, 3222–3230.
(28) Takaoka, K.; Maeda, S.; Miura, H.; Endo, K.; Chong, D. P. *Bull. Chem. Soc. Jpn.* **1998**, *71*, 807–816.
(29) Hallas, G.; Paskins, K. N.; Waring, D. R.; Humpston, J. R.; Jones, A. M. *J. Chem. Soc., Perkin Trans. II* **1977**, 450–456.
(30) Baraldi, I.; Carnevali, A.; Momicchioli, F.; Ponterini, G. *Chem. Phys.* **1992**, *160*, 85–96.
(31) Shandura, M. P.; Poronik, Y. M.; Kovtun, Y. P. *Dyes Pigm.* **2005**, *66*, 171–177.
(32) Prest, W. M., Jr.; Luca, D. J. *J. Appl. Phys.* **1979**, *50*, 6067–6071.
(33) Morino, S.; Machida, S.; Yamashita, T.; Horie, K. *J. Phys. Chem.* **1995**, *99*, 10280–10284.

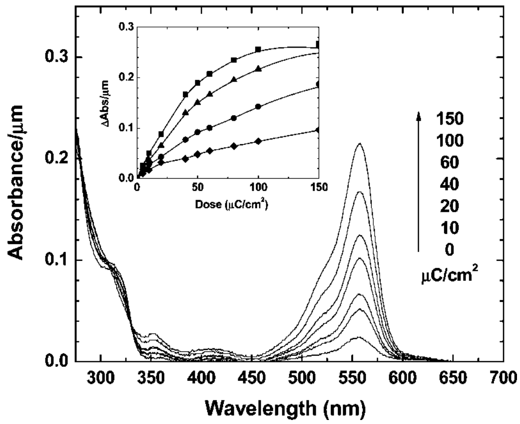

Figure 1. UV spectral changes of **RB/AG1(1/1)** irradiated upon EB with irradiation doses in the range from 0 to 150 μC cm^{-2}. (Inset) Absorbance changes (ΔAbs μm^{-1}) at 560 nm: (●) **AG1**, (▲) **AG2**, (■) **AG3**, and (◆) without acid generator.

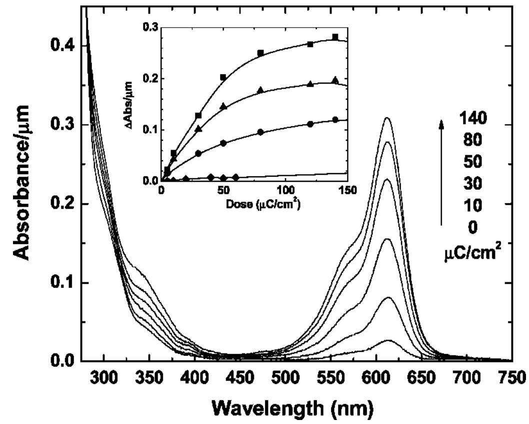

Figure 2. UV spectral changes of **BH/AG3 (3/3)** irradiated upon EB with irradiation doses in the range from 0 to 140 μC cm^{-2}. (Inset) Absorbance changes (ΔAbs μm^{-1}) at 612 nm: (●) **AG1**, (▲) **AG2**, (■) **AG3**, and (◆) without acid generator.

kept at 20 keV. The beam diameter was 50 nm with a probe current of 200 pA. The probe current was calibrated using a Faraday cup before and after experiments. Dose-dependent studies were performed with exposure doses of 4−150 μC cm^{-2}. Scanning color images were acquired using a KEYENCE VK-8500 digital microscope and using a Lasertec 1LM21H confocal scanning laser microscope.

Results and Discussion

EB-Induced Acid Chromism. A PMMA film consisting of **RB**, 1 wt % of the PMMA, and phenyl *p*-toluenesulfonate (**AG1**) equimolar to **RB** was prepared by spin coating on a quartz plate; it is referred to in this work as **RB/AG1(1/1)**. A film with a 0.61 μm thickness was obtained, and this was irradiated with an EB of 1 MeV at 1 mA with an exposure dose up to 150 μC cm^{-2} under air atmosphere. Figure 1 shows the UV spectral changes when the film was irradiated with doses in the range from 10 to 150 μC cm^{-2}. The intensity of the characteristic absorption band with λ_{max} at 560 nm gradually increased with increasing irradiation dose. The maximum value of ΔAbs was 0.19 μm^{-1} at 150 μC cm^{-2}. During irradiation, the appearance of the film changed from colorless to pale red. The PMMA film of **RB** and equimolar methanesulfonic acid (MsOH) had almost the same absorption spectrum with λ_{max} at 560 nm (see Figure S1 in the Supporting Information). Judging from this observation as well as the absorption maxima in the literature,[27,28] the new absorption maxima at 560 nm is assigned to the protonated form (**RB-H**$^+$) of **RB**. The spectral change in Figure 1 clearly shows two isosbestic points at 280 and 332 nm with a dose up to 150 μC cm^{-2}. This indicates that colorless **RB** in PMMA was transformed selectively to the protonated red **RB-H**$^+$ form without side reactions (Scheme 1).

Since the color-forming efficiency of chromic dyes in polymer films should be influenced by the acid generation efficiency of acid generators, PMMA films containing **RB** with equimolar 1,2,3-tris(methanesulfonyloxy)benzene (**AG2**) or triphenylsulfonium triflate (**AG3**) were prepared.[17–25] The changes in absorption spectra were monitored, and the absorption changes (in ΔAbs) at 560 nm are plotted as a function of exposure dose in the inset of Figure 1. The ΔAbs at 560 nm of the films with **AG2** and **AG3** increased with increasing irradiation dose, both reaching a maximum value of 0.26 μm^{-1} at around 150 μC cm^{-2}, which was higher than that with **AG1**. This difference can be attributed to the fact that the EB-induced acid generation rates of **AG2** and **AG3** were larger than that of **AG1**. These films with various acid generators had similar maximum values of ΔAbs at 560 nm, indicating that a desired quantitative degree of transformation from **RB** to **RB-H**$^+$ can be achieved by utilizing appropriate exposure doses. A PMMA film containing **RB** without any acid generators exhibited some increase of absorption at 560 nm (ΔAbs = 0.096 μm^{-1}) with a dose of 150 μC cm^{-2}. This color formation is attributed to the EB-induced formation of carboxylic acid, resulting in the radiolysis of PMMA; however, the maximum value of ΔAbs is less than one-half that of the films containing acid generators.

Bis(aminoaryl)methanol dyes such as **BH** undergo acid-catalyzed dehydration, resulting in conjugated ammonium cation structures,[29–31] and therefore can be used as an acid-chromic dye for color formation. PMMA film consisting of 3 wt % **BH** and equimolar **AG3** was prepared; it is referred to in this work as **BH/AG3(3/3)**. This film was obtained with 0.71 μm thickness and irradiated by the method mentioned above. Figure 2 shows the UV spectral changes when the film was irradiated with irradiation doses in the range from 10 to 140 μC cm^{-2}. The intensity of the characteristic absorption band with λ_{max} at 612 nm increased with increasing irradiation dose. The maximum value of ΔAbs was 0.28 μm^{-1} at 140 μC cm^{-2}. During irradiation, the appearance of the film changed from colorless to blue. Contrary to the case of **RB**, PMMA films of **BH** with MsOH could not be cast on a silicon wafer. This is probably due to the water molecules generated by the dehydration reaction of **BH** in the solution before spin coating. On the other hand, the dichloromethane solution of **BH** with MsOH has almost the same absorption spectrum with λ_{max} at 612 nm (see Figure S2 in the Supporting Information). Judging from this observation, the new absorption peak at 612 nm is assigned to the dehydrated form (**BH-H**$^+$) of **BH**.[29–31] The spectral change in Figure 2 clearly shows an isosbestic point at 280 nm with a dose up to 140 μC cm^{-2}, indicating that colorless **BH** in PMMA was transformed selectively to the protonated blue **BH-H$^+$** form without side reactions by a dose of at least 140 μC cm^{-2} (Scheme 1).

As with **RB**, the color-forming efficiency of an acid-chromic dye **BH** in polymer films was examined using equimolar **AG1**, **AG2**, and **AG3**. The changes in absorption spectra were monitored and the changes in absorption (ΔAbs) at 612 nm were plotted as a function of exposure dose in the inset of Figure 2. The ΔAbs at 612 nm of the films with **AG1** and **AG2** increased with increasing irradiation dose, reaching the maximum value of 0.20 and 0.12 μm^{-1}, respectively, at around 140 μC cm^{-2}. The ΔAbs of the films with **AG1** and **AG2** reached the saturated values with about 70% and 40% of the **BH/AG3(3/3)** film (0.29 μm^{-1}). This behavior can be attributed to the fact that the rates of EB-induced acid generation with **AG1** and **AG2** were lower than that of **AG3**; thus, the degradation reactions of the resulting **BH-H$^+$** became noticeable with doses higher than 150 μC cm^{-2} in the films with **AG1** and **AG2**, which required higher irradiation doses for their consumption. The ΔAbs values of the PMMA film containing **BH** without any acid generator were less than 0.02 μm^{-1} with a dose up to 300 μC cm^{-2}. The different result of these blank experiments with **RB** and **BH** indicates that the acidity of the carboxylic acids generated from PMMA by EB-induced degradation is not high enough to cause dehydration of **BH** and generate **BH-H$^+$**, so that in this case there is almost no color formation in the film.

EB-Induced Color Imaging. The EB-induced color formation of PMMA with acid-chromic dyes and acid generators could be applied to nanoscale color imaging using EBDW. The color imaging of 5 μm square patterns and 100−1000 nm line and space patterns on the **RB/AG1(1/1)** film (0.35 μm thickness) was performed using EBDW with a 50 nm diameter beam and evaluated by optical and confocal laser microscopy. Figure 3a shows the optical microscopic images of a pattern of 5 μm squares on **RB/AG1(1/1)** film made with a dose of 30 μC cm^{-2}. Although the shape of the image is somewhat blurred, the pale red pattern can be observed. As shown in Figure 3b, the confocal scanning laser micrographs of the same film exhibit much better resolution after EBDW with a dose of 100 μC cm^{-2}. Clear black and white patterns can be observed on the irradiated film with resolutions of 300 nm in square patterns and 200 nm in line/space patterns. In other words, the **RB/AG1(1/1)** film can be printed with line/space patterns by EBDW having a resolution of 300 nm.

The color-forming efficiency of **BH** in a film is lower than that of **RB**. Thus, more **BH** and acid generators were introduced to the film to enhance its sensitivity to EB; specifically, PMMA film consisting of 3 wt % **BH** and 3-fold molar **AG3** relative to **BH** (**BH/AG3(3/9)**) was prepared. Figure 3c shows optical microscopic images of **BH/AG1(3/9)** film with a dose of 30 μC cm^{-2}, resulting in a pattern of 5 μm squares. A clear blue color image of 5 μm squares can be observed. As shown in Figure 3d, the confocal scanning laser micrographs of the same film have clear images with higher resolution (100−200 nm) after a dose of only 10 μC cm^{-2}. The **BH/AG1(3/9)** film pattern possesses higher sensitivity and resolution than that of **RB/AG1(1/1)** film after EBDW because of the higher content of acid-chromic dyes and acid generators in the PMMA film. Judging from the above observations, the sensitivity of the acid-induced color change is further enhanced by increasing the added amounts of both acid-chromic dyes and acid generators. A film with even 10 wt % acid-chromic dye and 10 times excess acid generator still exhibits good film-forming properties.

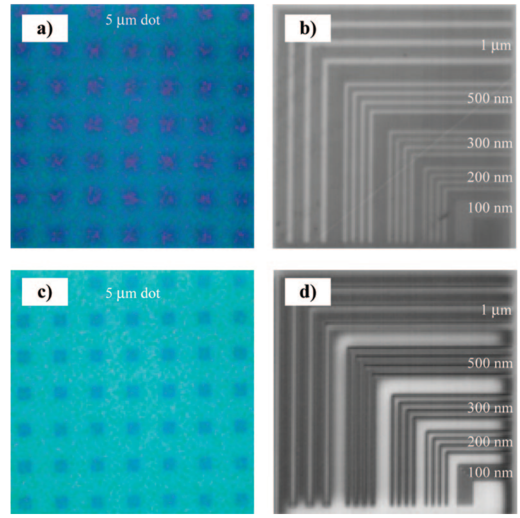

Figure 3. Images of acid-induced color change polymer films with optical differentiation between the exposed and unexposed regions provided by electron-beam direct writing. (a) Optical microscopic image of a pattern of 5 μm squares on **RB/AG1(1/1)** film made with a dose of 30 μC cm^{-2}. (b) Confocal scanning laser micrographs with a dose of 100 μC cm^{-2} for line/space patterns with 100−1000 nm. (c) Optical microscopic image of a pattern of 5 μm squares on **BH/AG1(3/9)** film made with a dose of 30 μC cm^{-2}. (d) Confocal scanning laser micrographs with a dose of 10 μC cm^{-2} for line/space patterns with 100−1000 nm.

The black and white image of the **BH/AG3(3/9)** film was inversed from that of the **RB/AG1(1/1)** film. Since blacker and whiter images of films show higher and lower light intensities at 632.8 nm according to the principle of a black/white contrast measurement mode of confocal microscopy, the light intensity of the **RB/AG1(1/1)** film increases while that of the **BH/AG3(3/9)** film decreases after irradiation. The different change in absorption at 632.8 nm in the films with **RB** and **BH** might be the reason why the light intensities of these films were inversed from each other after irradiation.

Refractive Index Studies. To elucidate the reason why confocal laser microscopy revealed thinner lines than the optical resolution limit determined by the laser wavelength (632.8 nm), the refractive indices of acid-chromic polymer films at 560 nm before and after EB irradiation were determined for the TM and TE modes by m-line measurement (Figure 4).[32,33] The refractive index of **RB/AG1(1/1)** linearly increased from 1.492 to 1.505 in the TE mode with increasing irradiation dose up to 80 μC cm^{-2}. As shown in Figure 4, the linear relation between the refractive index and the absorbance suggests that the refractive index change of these films results from the appearance of a new absorption at a longer wavelength than in the original films. Accordingly, the large change of refractive index of these films

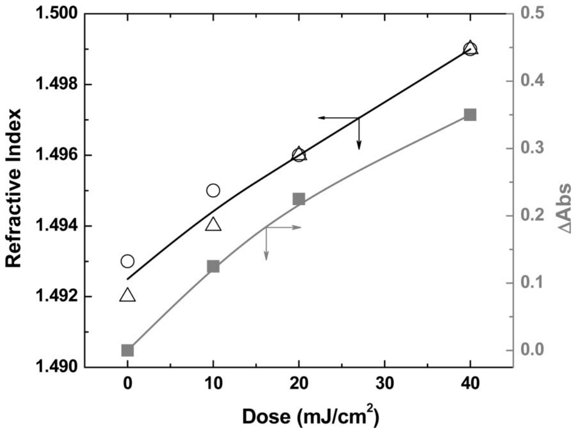

Figure 4. Relationship between refractive index and absorbance change at 560 nm of **RB/AG1 (1/1)** film as a function of irradiation doses: (○) and (Δ) refractive index changes in TE and TM mode (Δn_{TE} and Δn_{TM}); (■) absorbance change (ΔAbs) at 560 nm in the right-hand axis.

induced by EB irradiation even at a low energy dose should be the main factor enabling the clear confocal laser micrographs with a resolution thinner than the optical resolution limit. Furthermore, no significant difference between n_{TE} and n_{TM} was observed over the whole range of irradiation doses, indicating that the acid-chromic polymer films had little birefringence with or without EB irradiation. The EB-induced refractive index changes of both modes were very large ($\Delta n_{TE} = 0.013$, $\Delta n_{TM} = 0.012$), sufficient to create an optical circuit with a relatively small irradiation dose. At this time it is very difficult to estimate the resolution limit of the films. However, the limit seems to be dependent on observation methods rather than EBDW methods. Increases in the amount of acid-chromic dyes as well as acid generators did not decrease the resolution limit, at least where the resolution was on the scale of 100 nm or more as in this experiment.

Conclusions

We designed and prepared polymer films containing an acid generator and acid-chromic dyes which can be converted from colorless to colored forms by complexation with acids generated from acid generators. Nanoscale color imaging can be conducted on these films by EBDW without post-treatment such as color-forming chemical reactions and thermal transformations. PMMA films containing **RB** and **AG1** (**RB/AG1(1/1)**) exhibited a characteristic absorption band with λ_{max} at 560 nm and an isosbestic point upon EB irradiation. These spectral changes clearly show that colorless **RB** in PMMA was transformed selectively to the protonated red **RB-H$^+$** form. PMMA film containing **BH** and **AG3** (**BH/AG3(3/3)**) exhibited a characteristic absorption band with λ_{max} at 612 nm and an isosbestic point upon EB irradiation. A spectral change similar to that of **RB/AG1(1/1)** indicates the quantitative transformation from colorless **BH** to the protonated blue **BH-H$^+$** in PMMA. The color imaging of the **RB/AG1(1/1)** and **BH/AG3(3/9)** films with 100−1000 nm line and space patterns was performed by direct writing with a 50 nm diameter beam. In the confocal laser microscopic image, the **RB/AG1(1/1)** film exhibited clear color imaging with a resolution of 200 nm after irradiation with 30 μC cm^{-2}. Furthermore, a **BH/AG3(3/9)** film, which had a greater amount of acid-chromic dye and acid generator, exhibited color imaging with higher resolution (100−200 nm) after a dose of only 10 μC cm^{-2}. The reason why the confocal laser microscopy revealed thinner lines than the optical resolution limit determined by the laser wavelength (632.8 nm) may be the large change of refractive index of these films induced by EB irradiation even at a low energy dose, which were determined for TM and TE modes by m-line measurement.

Supporting Information Available: UV absorption spectra of RB and BH with methanesulfonic acid (MsOH) (PDF). This material is available free of charge via the Internet at http://pubs.acs.org.

CM800650Q